

THE EFFECT OF MULTIPLE ISOTHERMAL FORGING ON THE STRUCTURE AND MECHANICAL PROPERTIES OF LOW CARBON STEEL 12GBA AND ON THE FRACTURE PROCESS AND ITS CHARACTERISTICS

L.S. Derevyagina^{1,a}, A.V. Korznikov^{2,b}, L.V. Zatochnaya^{1,c}, I.M. Safarov^{2,d}

¹Institute of Strength Physics and Materials Science, SB RAS, Tomsk, Russia

²Institute of Metals Superplasticity Problems, RAS, Ufa, Russia

^a lsd@ispms.tsc.ru, ^b korznikov@imsp.da.ru, ^c ivanovskaya.l@gmail.com,

^d ilfat@anrb.ru

Keywords: isothermal multidirectional forging, steel, ultrafine grain structure, texture, fracture micromechanisms, impact viscosity.

Abstract. An in-depth study was made of the grain-subgrain structure of steel 12GBA, which had been treated by multiple isothermal forging (MIF); the fracture behavior of material was also examined. The investigations were performed using the methods of electron microscopy, back-scattered electron diffraction as well as metallographic, X-ray and fractographic analyses. The formation of an ultrafine grain structure causes a three-fold increase in the yield stress of material, which becomes close to its ultimate tensile strength. As a result, the liability of material to plastic flow localization would become more pronounced. Due to the formation of localized plasticity macro-band, the plasticity and fracture behavior of material are impaired significantly. As-treated steel will exhibit low-temperature brittleness at temperatures that are 20°C lower relative to the coarse-grain counterpart. The impact toughness y of as-treated steel observed in the temperature interval from -45°C to -200°C is higher relative to that of the coarse grain counterpart.

Introduction

Among the traditionally employed construction materials low carbon steels having low alloying addition content have wide application. The most general requirements imposed on steels are enhanced strength, high corrosion resistance, satisfactory weldability and low susceptibility to embrittlement. Grain refinement is known to suppress material susceptibility to cold embrittlement. One of the most promising methods for obtaining a fine grain structure is severe plastic deformation (SPD) [1]. The effect of SPD on the structure and strength characteristics of steels having low alloying addition contents is reported in the literature [2-3]. However, the implementation of SPD methods would require expensive equipment; besides, a limitation is imposed on billet size. Thus a demand has been created for SPD methods using traditional technologies of metal working, e.g. forging.

The goal of the given study is an investigation of steel 12GBA treated by MIF in isothermal conditions in order to define its structure, mechanical properties and the of ductile-to-brittle transition temperature T_c ; matching of the parameters obtained with those of the coarse grain counterpart.

Material and Investigation Methods

The chemical composition of the investigated steel is illustrated in Table 1. The steel was worked by MIF on a hydraulic press in isothermal conditions: both the striker and the billet were heated at each successive step to 700°C, 600°C and 500°C. The scheme employed is described elsewhere [4]. The original samples had dimensions of 20×30×40 mm; the total true reduction

$\varphi=6.2$. Four upsets were performed to a 40% reduction at each step of deformation. The final

Table 1. Chemical composition of steel 12GBA

| Alloying addition content, % by weight | C | Mn | Si | Nb | Cu | Al | S | P |
|---|------|-----|------|------|------|--------|-------|--------|
| 12GBA | 0.11 | 1.2 | 0.25 | 0.05 | 0.35 | 0.0026 | 0.005 | 0.0012 |

upset of the billet was carried out at 450°C to give a disk having diameter ~80 mm and thickness ~8 mm. A scheme of cutting out samples for mechanical tests is illustrated in Fig. 1.

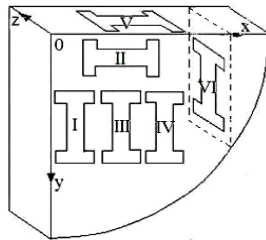


Fig.1. A scheme of cutting out test samples (oz – direction of final upset).

The structural and phase investigations were conducted on an optical microscope ‘Zeiss Axiovert 25’, a transmission electronic microscope ‘JEM-2000EX’ and a raster electronic microscope ‘Carl Zeiss EVO 50’ having an attachment ‘NORDLYS’ (Oxford Instruments HKL Technology) intended for analysis of back-scattered electrons diffraction (EBSD). The analysis of material fracture was performed on a raster electronic microscope ‘SEM 515’ (Philips). The X-ray investigations were conducted on a diffractometer ‘DRON-4M’ in $Co_{K\alpha}$ radiation. A comparative assessment of fracture energy was made for the test samples of steel in the ultrafine grain, coarse grain and tempered coarse grain states. The impact tests were carried on in the temperature interval of 20°C to -200°C, using a pendulous impact testing machine ‘Tinius Oisen 1T542M’. The test samples had dimensions 10×10×15mm; each had a V-notch 1.5 mm deep.

Experimental Results

The structure of steel 12GBA. The original material had coarse grain structure containing near-equiaxial ferrite grains (average size 25 μm) and uniformly distributed pearlite colonies (volume fraction 13.5 %). The steel treated by MIF still retains ferrite-pearlite streakiness, which may be partly due to liquation non-uniformity caused by the crystallization and subsequent mechanical treatment of as-received material. The degree of deformation of as-treated material is $\geq 70\%$; the material in sections showing the direction of final upset has a forging texture which is distinguished by ferrite-pearlite streakiness and by an elongated shape of crystallites (Fig. 2, section zoy).

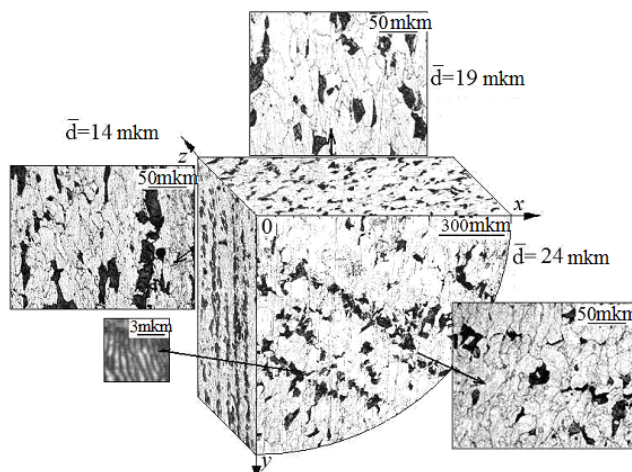


Fig. 2. Structure of steel 12GBA treated by MIF.

The structure of steel treated by MIF is found to contain pearlite lines (surfaces *yox* and *zoy*), with the separation between the lines varying from 37 to 50 μm . The averaged grain size \bar{d} obtained for three surfaces of α -iron is 19 μm . The morphology of granular structure has certain distinctive features which vary from section to section. Thus non-equiaxiality coefficient L/d of 1.66 has been obtained for the granular structure (section *zoy* in which lies the direction of final upset). This value is suggestive of significant shape anisotropy of grains due to incomplete dynamic recrystallization of material.

The electron microscopic images reveal the occurrence in the ferrite phase of granular structure fragments having sizes 0.3-0.5 μm (Fig. 3). This suggests that in steel 12GBA treated by MIF has formed an ultrafine grain structure, which shows a significant shape anisotropy of grain fragments (sections *zoy* in which lies the direction of final upset in Fig. 3b). This finding is validated by EBSD data (Fig. 4). Grain fragment width in the latter sections is about half that of the sections orthogonal to the direction of final upset (Table 2).

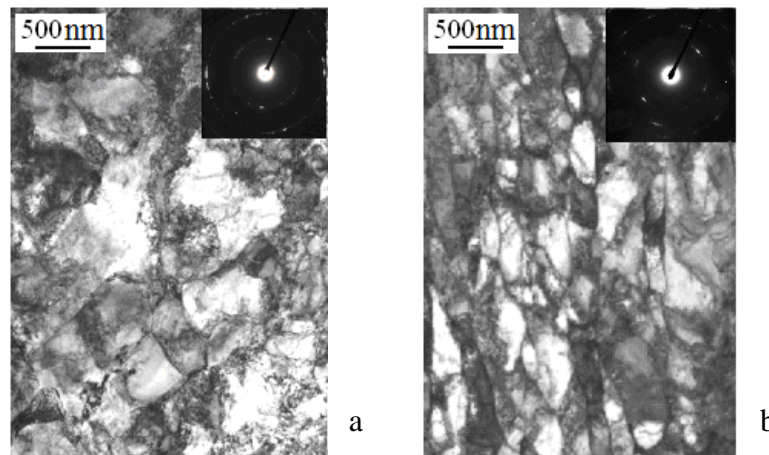


Fig.3. Structure of steel 12GBA treated by MIF in sections *yox* (a) and *zoy* (b).

Steel 12GBA treated by MIF contains a greater fraction of low-angle boundaries relative to as-received material (Table 2). The EBSD data suggests the occurrence of a two-component axial texture $\langle 111 \rangle + \langle 100 \rangle$ in the ferrite phase of section *yox*, with the intensity of component $\langle 111 \rangle$ prevailing insignificantly (Fig. 5). In the course of MIF treatment dissipative processes are liable to occur which would cause crystal structure defects; therefore, the microstructure of as-treated steel 12GBA was examined by an X-ray method.

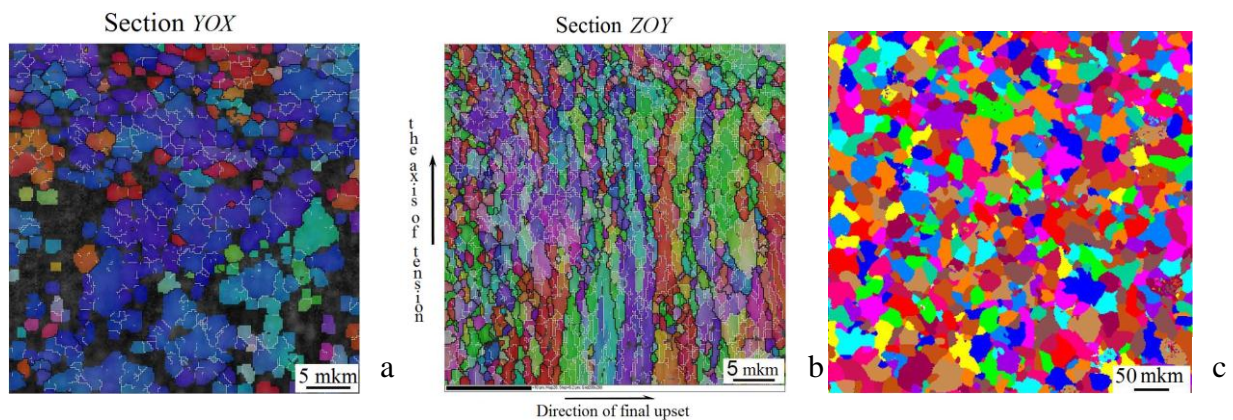


Fig.4. EBSD data on the structure of steel 12GBA in ultrafine grain (a, b) and coarse grain state (c).

Table 2. Granular structure and grain boundary state of steel 12GBA

| material state | HAB, % | LAB, % | grain size d, μm |
|-----------------------|--------|--------|-----------------------------|
| coarse grain | 12 | 88 | 25 |
| tempered coarse grain | 15.4 | 84.6 | 0.98; 1.34 |
| Type I | 73.6 | 26.4 | 1.06; 1.12 |
| Type II | 83.7 | 16.23 | 1.04; 1.54 |
| Type V | 73 | 27 | 0.54; 0.61 |
| Type VI | 74 | 26 | 0.65; 0.82 |

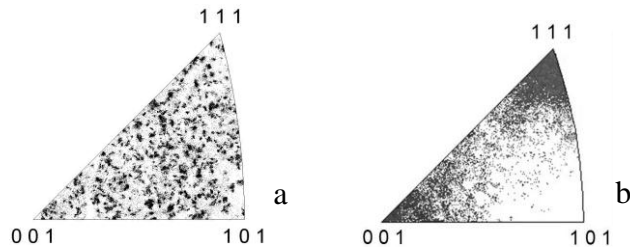


Fig.5. Inverse pole figures coarse grain grain state (a) and ultrafine grain state in section yox (b).

Using an X-ray method, the lattice constant was measured for the ferrite phase of coarse grain and ultrafine grain material; the values obtained are $a=2.8672 \text{ \AA}$ and $a=2.8669 \text{ \AA}$, respectively. With allowance made for measurement error, the latter two values are close to the respective value obtained for pure α -iron, i.e. $a=2.8664 \text{ \AA}$. This suggests that the carbon atoms occur in the pearlite or carbides rather than in the solid ferrite solution. The X-ray data also suggests that the MIF treatment would cause elastic distortions of the lattice; consequently, the microstrain ε is liable to increase in the ultrafine grain steel by 4-5 times relative to the coarse grain counterpart. Moreover, the dislocation density of the former material is found to increase by one order; the value obtained is $5.2 \times 10^9 \text{ cm}^{-2}$.

The tempered coarse grain steel has a more disperse and homogeneous structure; its microhardness \bar{H} is twice that of the original coarse grain counterpart, i.e. 1.55 and 0.78 GPa, respectively. However, the highest microhardness is observed for ultrafine grain steel, i.e. $\bar{H}=2.24 \text{ GPa}$

Mechanical properties of steel 12GBA

Due to the formation of ultrafine grain structure in steel treated by MIF, a three-fold enhancement in the yield stress is achieved; besides, the ultimate tensile strength of the ultrafine grain steel is one and a half that of the coarse grain counterpart (Fig. 6). The flow stress values obtained for test samples cut out from different sections of the billet differ by $\sim 18\%$.

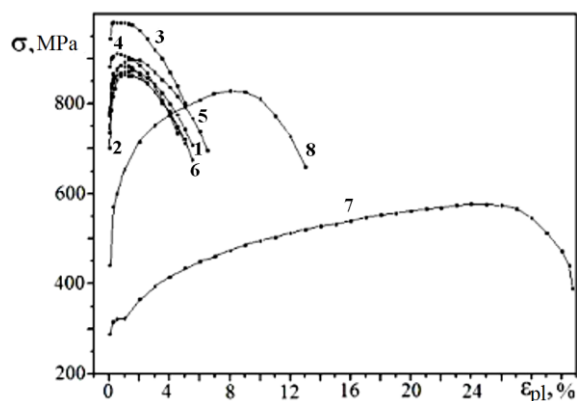


Fig.6. Stress-strain diagrams of steel 12GBA in ultrafine grain, coarse grain and tempered coarse grain state (samples 1 through 6, 7, 8, respectively).

The fracture behavior of steel 12GBA

The steel treated by MIF is prone to the formation of localized plasticity macrobands, which

significantly impairs its plasticity and affects its fracture behavior. The steel samples cut out from section yox would undergo macrofracture by cross shear at 60° to the extension axis. The fracture surface shows deep delaminates (Fig. 7b) having smooth walls and clearly defined relief, which mirrors the pattern of lamellar cellular structure (Fig. 7c) similar to that of the substructures in section zoy (Figs. 3b and 4b). Traces of ductile fracture are found to occur in the areas in between the delaminates. In a number of areas there are indications of intergranular fracture (Fig. 7d), with the dimple diameter $1-3 \mu\text{m}$, which is comparable to the grain size of ultrafine grain structure. The material in sections zox and zoy undergoes fracture by longitudinal shear along the localization macroband at 60° to the extension axis, with the fracture surface showing no large delaminates. The lens-shaped macrofracture trajectories occurring on the face of coarse grain steel samples are suggestive of ductile fracture. The fracture surface is matted and dimpled in places; therefore, the fracture micromechanism is termed as ‘dimpling’. The dimple diameter is $10-50 \mu\text{m}$, which is also comparable with the grain size of material (Fig. 7a). Some dimples contain spherical $5 \mu\text{m}$ -particles; their occurrence suggests that the fracture micromechanism involves retardation of dislocations by secondary-phase particles.

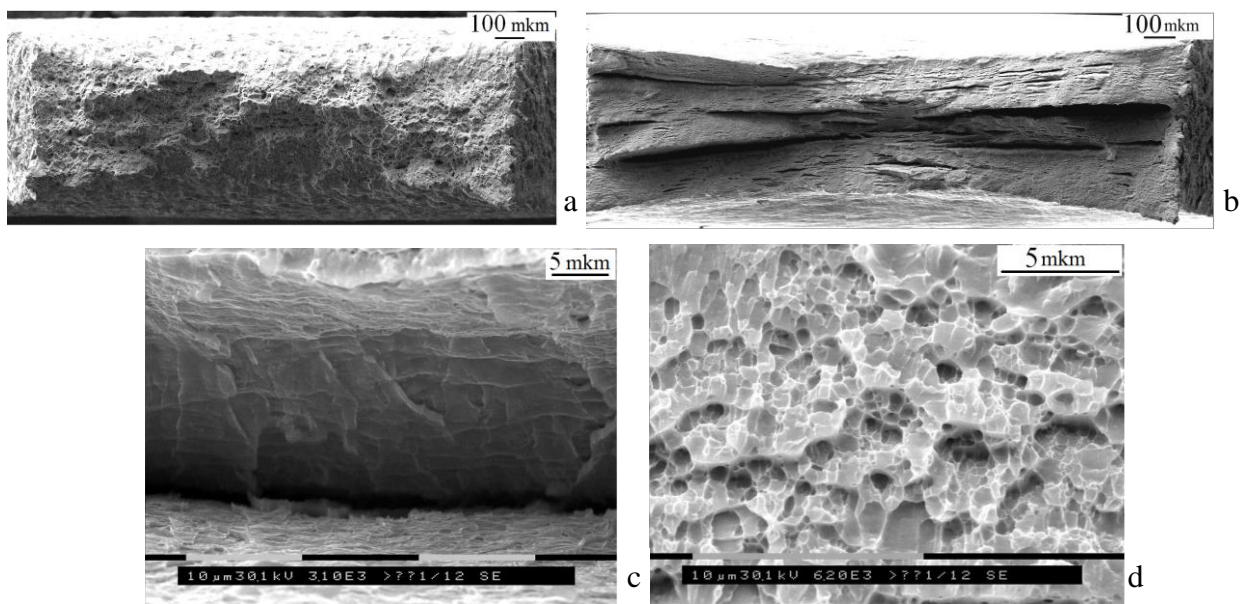


Fig.7. Fracture surface of steel 12 GBA in coarse grain (a) and ultrafine grain state (b, c, d).

The main emphasis is on the fracture toughness of steel; therefore, the impact toughness KCV and the ductile-to-brittle transition temperature T_c were determined for the investigated steel. The impact toughness is known to characterize the expenditure of energy for fracture. A series of KCV curves obtained for steel 12GBA are demonstrated in Fig. 8. The value T_c is taken to be the temperature corresponding to $KCV=0.25 \text{ MJ/m}^2$. Thus the values T_c obtained for the ultrafine grain and coarse grain counterparts are -80°C and -60°C , respectively.

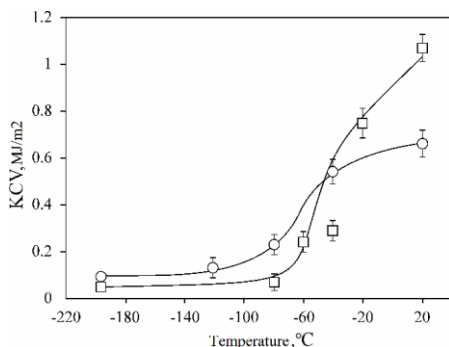


Fig.8. Temperature dependence of impact toughness KCV of steel 12GBA in coarse grain (□) and ultrafine grain state (○).

Thus, ultrafine grain steel would exhibit low-temperature brittleness at temperature that is 20°C

lower relative to the coarse grain counterpart. However, the value KCV observed for the former material in the temperature interval from 20°C to -45 °C is lower relative to the coarse grain counterpart, e.g. the corresponding values obtained at 20°C are 0.64 MJ/m² and 1.05 MJ/m², respectively.

Discussion of Results

As a result of MIF treatment, an ultrafine grain structure is formed in as-treated steel. The material in ultrafine grain state has an enhanced microhardness relative to as-received material, i.e. 2.24 and 0.78 GPa, respectively, which is mainly due to grain refinement since the average size of grain-subgrain structure elements is 0.3-0.5 μm. Besides, the density of dislocations grows by one order and microdeformation ϵ increases by 4-5 times, which suggests a higher degree of elastic distortion of the crystal lattice. The structure of steel 12GBA treated by MIF has the following distinctive features. (i) In all the sections containing the direction of final upset the material structure has a clearly pronounced ferrite-pearlite streakiness and distinct shape anisotropy of grain-subgrain structure elements. (ii) The fraction of low-angle boundaries in all the sections grows significantly. (iii) In section yox orthogonal to the direction of final upset forms a two-component axial texture $\langle 111 \rangle + \langle 100 \rangle$ that is typical of compressive bcc material samples [5]. An enhancement in the strength properties of steel treated by MIF is chiefly attributed to the effect of subgrain boundary strengthening. The flow stress is found to differ by ~18% for samples cut out from different sections, which must be due to shape anisotropy of grain-subgrain structure elements.

It is believed that the only effective strengthening mechanism is that of subgrain boundary strengthening, which also enhances fracture toughness of steels [1,6]. Indeed, the effects of MIF treatment encompass a considerable range: due to grain refinement, grain/subgrain structure elements would reveal shape anisotropy and a change in the type of grain boundaries would occur; besides, the degree of elastic distortion of the lattice would increase, the density of dislocations would grow and a new texture would form. The MIF treatment of material would result in an increase in the yield stress $\sigma_{0.2}$ which becomes close to the ultimate tensile stress σ_B ; consequently, the material is prone to plastic flow localization. Moreover, the occurrence of delaminates in as-treated steel may affect its fracture toughness. The above factors would affect the energy of fracture, although to a different degree; therefore, the fracture behavior of steel in an ultrafine grain would differ significantly from that of the coarse grain counterpart.

In what follows the structural features responsible for the occurrence of delaminates are considered in greater detail; the effect of delaminates on the fracture toughness of steel is also discussed. The following structural features are thought to be responsible for the occurrence of delaminates in steels [7]: (i) nonmetallic inclusions; (ii) inclusions of AlN, CaS and MnS and of carbides of microalloying Ti, V, Nb and Mo additions; (iii) ferrite embrittlement due to the occurrence on the grain-boundaries of monoatomic segregations of active P, Sb, Sn and As impurities; (iv) the line-like form of ferrite, pearlite, bainite and martensite structure elements; (v) the occurrence of crystallographic mesostructure. A different opinion is put forward in [8]; the formation of delaminates in metals is assumed to be related to the occurrence of high internal stresses on the boundaries of layered cellular elements which are aligned parallel to the rolling plane.

It is pointed out above that the structure of steel 12GBA treated by MIF has ferrite-pearlite streakiness. Similar investigations were carried on for α -iron in ultrafine grain state in which delaminates were also observed although the material contained no pearlite [9]. This indirectly suggests that ferrite-pearlite streakiness is not responsible for the occurrence of delaminates. The structural investigations revealed no significant change in the distribution of nonmetallic carbonitride inclusions in steel GBA treated by MIF. This leads us to conclude that the delaminates having smooth surface might be due to the occurrence of meso-scale areas in which material has cubic orientation. The available data suggests that the occurrence of such areas might be the cause of delaminates in bcc iron. In accordance with the Cottrell dislocation model,

cubic texture will favor crack initiation. The electron images and EBSD patterns obtained for the investigated steel (Figs. 3b and 4b, respectively) suggest that the occurrence of delaminates might be also due to the formation of layered cellular structure. The validity of this contention is supported by a fracture pattern, which has a layered cellular relief mirrored on the smooth walls of delaminates (Fig. 7c).

There is no consensus of opinion among the authors regarding the effect of delaminates on the fracture toughness of steels [7, 10-17]. Thus some workers regard the occurrence of delaminates as an indication of impaired fracture toughness of material [7, 10, 11], while the others believe, on the contrary, that the delaminates occurring along the weakened surfaces are liable to change the stressed state at the apex of main crack to a less rigid plane stress state, which would cause an enhancement in the fracture toughness of material [12-14]. A group of investigators argue along the same lines: they maintain that the technological and service properties of steels are unaffected by the occurrence of delaminates and that the occurrence of delaminates on the fracture surface is an indication of satisfactory fracture toughness of steel at the temperature of item functioning [15]. The examination delaminates occurring in steel samples suggests that an enhancement in the fracture toughness might be attributed to a prevalence of cubic components in the texture $\{100\} \langle 110 \rangle$ of material; in the case of other textures, however, the fracture toughness would decrease [16]. In any case, it is maintained that delaminates are deleterious defects, since they are liable to cause corrosion. Besides, the occurrence of delaminates in steels and iron base alloys would set a limit on the thermal treatment conducted to a high degree of reduction of the treated items [8]. The exposure of such steel to a corrosive medium cannot be tolerated since its high fracture toughness is due to the dissipation of energy caused by the opening of delaminates rather than to the state of material as such [17].

An enhancement in the strength characteristics of the ultrafine grain steel relative to the coarse grain counterpart might affect the rigidity of stressed state by fracture, thereby decreasing the expenditure of fracture energy.

Due to the occurrence of high elastic distortions of the lattice, the fracture toughness of steel treated by MIF might decrease, which is liable to initiate crack nucleation in the same. It is a well-established fact [18] that plastic flow localization is likely to decrease the energy of ductile fracture. It is noted above that the yield stress of ultrafine grain steel is close to its ultimate tensile strength, i.e. $\sigma_{0.2}/\sigma_B \sim 0.95$, which enhances the tendency of the material to deformation localization and fracture. Ultrafine grain steels are prone to decohesion within localized deformation zones, which is expected to decrease the expenditure of fracture energy.

It is known that low-angle boundaries and boundaries having high density of coincident nodes have low energies; the lower the energy of boundaries, the less impurity is segregated on the same. Hence processes involving intergranular embrittlement would preferentially occur in materials having high-angle boundaries. It is therefore concluded that due to the growing fraction of low-angle boundaries, the fracture toughness of ultrafine grain steel might increase.

It has proved difficult to find unambiguous evidence for the influence of MIF treatment on the fracture toughness of as-treated steel. The temperature dependencies of fracture toughness and the ductile-to brittle transition temperatures were matched for the ultrafine grain and coarse grain counterparts. It has been found that the impact toughness observed at room temperature for the coarse-grain counterpart is 1.6 that of the ultrafine grain counterpart. This finding agrees with the results of fractographic analysis, which suggest that samples of ultrafine grain steel have a greater number of areas in which material undergoes intergranular embrittlement relative to the coarse grain counterpart. This leads us to conclude that ultrafine grain steel has lower expenditure of fracture energy relative to the coarse grain counterpart. However, the impact toughness observed for steel treated by MIF at low temperatures is higher and the ductile-to brittle transition temperature T_c is lower relative to the coarse grain counterpart. An enhancement in the strength properties of ultrafine grain steel might increase its crack propagation resistance, which will cause the value T_c to decrease, and, consequently, increase the resistance of material to low-temperature embrittlement.

Conclusions

- (1) Steel 12GBF treated by MIF has an ultrafine grain structure characterized by the occurrence of ferrite fragments having size 0.3 μm , microdeformation $\varepsilon \sim 0.02\%$ and a higher fraction of low-angle boundaries relative to the coarse grain counterpart. The structural features of material are distinguished by the ferrite-pearlite streakiness and by the shape anisotropy of grain-subgrain ferrite structure elements.
- (2) The yield stress of as-treated steel is three times relative to the coarse grain counterpart; its ultimate tensile strength is 1.5 times that of as-received material.
- (3) Steel treated by MIF is prone to plastic flow localization, which impairs significantly its ductility and determines its fracture behavior.
- (4) The delaminates observed in the fracture surfaces are probably due to the occurrence of high stresses on the boundaries of layered cellular structure as well as to the axial texture $\langle 111 \rangle + \langle 100 \rangle$, which favors crack nucleation by the Cottrell mechanism.
- (5) Steel 12GBA in an ultrafine grain state has an enhanced impact toughness KCV at temperatures below zero; the ductile-to brittle transition temperature T_c is 20°C lower relative to as-received material. However, the value KCV observed in the temperature interval of 20°C to -45°C is slightly lower relative to the coarse grain counterpart.
- (6) The efficiency of MIF treatment might be enhanced provided the original material has a more homogeneous structure; the degree of reduction in the course of final upset should be decreased and anneals should be performed in less severe conditions to decrease elastic stresses on the layered cellular boundaries.

References

- [1] N.J. Petch: Atomic Fracture Mechanism (Metallurgizdat Publishers, USSR, Moscow 1963 in Russian).
- [2] S.P. Yakovleva, S.N. Makarov, M.Z. Borisova: Metals No. 4 (2006), p. 71
- [3] E.G. Astafurova et al., in: Metal Physics and Mater. Sci. Vol. 110 No. 3 (2010), p. 275
- [4] R.R. Mulyukov, R.M. Imayev, A.A. Nazarov: J Mater Sci. Vol. 43 (2008), p.7257
- [5] P.I. Polukhin, S.S. Gorelik, V.K. Voronov: Metallurgy (1982), p. 584
- [6] M.I. Goldstein, S.V. Grachev, Yu.G. Veksler, in: Special-Purpose Steels edited by MISIS Publishers, Moscow, Russia (1999).
- [7] A.B. Arabey et al.: Izvestiya VUZ. Iron Metallurgy No. 9. (2009), p. 9
- [8] V.I. Trefilov, Yu.V. Milman, S.A. Firstov, in: Physical Basis of Strength of High-Melting Metals, Naukova Dumka Publishers (1975).
- [9] L.S. Derevyagina, V.E. Panin, A.I. Gordienko: Physical Meso-Mechanics Vol. 10 No. 4 (2007), p. 59
- [10] A.B. Arabey, I.Yu. Pyshmintsev, M.A. Shtremel: Izvestiya VUZ. Iron Metallurgy No. 9 (2009), p. 3
- [11] N.V. Malakhov et al.: Mater. Sci. Problems Vol. 59 No. 3 (2009), p. 52
- [12] D.A. Mirzaev et al.: Deformation and Fracture in Materials No. 3 (2006), p. 24
- [13] D.A. Mirzaev et al.: Metal Physics and Mater. Sci. Vol. 98 No. 3(2004), p. 90
- [14] M.L. Berstein, P.D. Odessky, T.M. Grunvald: Izvestiya VUZ. Iron Metallurgy No. 11 (1972), p. 85
- [15] Yu.I. Matrosov, D.I. Litvinenko, S.A. Golovanenko: Metallurgy (1989), p. 289
- [16] V.M. Schastlivtsev et al.: Deformation and Fracture in Materials No. 11 (2010), p. 34
- [17] L.R. Botvina, in: Kinetics, Mechanisms and General Trends of Fracture, edited by Metallurgy and Mater. Sci. Institute Publishers/Nauka Publishing, Moscow, Russia (2008).
- [18] P.D. Odessky, in: Metal Fracture Problems and Fractography, Znanie Publishers, Moscow, Russia (1989).

